Available online at www.sciencedirect.com
ScienceDirect
Journal of the European Ceramic Society 28 (2008) 959–963
www.elsevier.com/locate/jeurceramsoc

Alumina/cerium oxide nano-composite electrolyte for solid oxide fuel cell applications

Rajalekshmi Chockalingam, Vasantha R.W. Amarakoon, Herbert Giesche *

New York State College of Ceramics at Alfred University, Alfred, NY, USA

Available online 26 October 2007

Abstract

Gadolinium-doped ceria has demonstrated a high-ionic conductivity at moderate temperatures and is a potential candidate as electrolyte in solid oxide fuel cell (SOFC) devices. However, Ce ions can undergo a valency change from +IV to +III under reducing conditions. That valency change then leads to electronic (polaron) conduction and thus, degrades the ionic conduction. It has been demonstrated that the incorporation of electrically insulating particles will reduce the electronic conduction by an 'electron-trapping' mechanism (ideally) without affecting the ionic conductivity. This design is principally similar to the grain boundary design in zinc-oxide varistors.

In order to make this design effective, the insulating (electron trapping) particles have to be spaced close to each other. The spacing between 50 and 100 nm is assumed to be necessary for optimum performance. In order to not overload the entire composition with insulating particles (and thus reducing the ionic conductivity substantially due to volumetric dilution) the insulating grains have to be small (nanometer sized) and uniformly distributed throughout the matrix (cerium oxide). Moreover, the insulating grains should not dissolve or otherwise alter the cerium oxide matrix.

The present study now focuses on the precipitation of nanometer-sized alumina particles and coating these 'seed' particles with a 50 nm layer of gadolinium-doped cerium oxide. Small sizes for the alumina particles will prevent the overall composition from being overloaded with non-conducting particles and the coating process will enhance a very uniform distribution of the alumina particles in the cerium oxide matrix. Afterwards, the powders were calcined, compacted and (microwave) sintered. Characterization by SEM, TEM, XRD, density, and conductivity measurements are presented to evaluate properties of the proposed nano-composite electrolyte.

Keywords: Solid oxide fuel cell; Electrolyte; Coated particles; Nano-composite

1. Introduction

In solid oxide fuel cells (SOFCs), a dense electrolyte membrane is sandwiched between two porous electrodes. The membrane serves as a barrier to gas diffusion, but will let ions migrate across it. A typical SOFC consists of 8 mol% Y_2O_3 stabilized ZrO_2 as the electrolyte, a ceramic–metal composite of Ni + YSZ as the anode and $La_{1-x}Sr_xMnO_{3-\delta}$, as the cathode ($x$ between 0.15 and 0.25) and typically operates at temperatures close to 1000 °C. Obviously it would be advantageous to use electrolyte membranes, which could be operated at lower temperatures, but with equivalent oxygen transport properties. Fig. 1 illustrates the properties of various alternative materials. However, one major problem is the fact that the ionic conductivity is compromised by electronic conductivity at these operation conditions. For example gadolinium-doped ceria has sufficient ionic conductivity at temperatures as low as 500–600 °C. However, Cerium ions are being reduced from +IV oxidation state to a +III oxidation state under the reducing conditions present at one side of the membrane. Thus, the material shows a significant electronic conductivity counteracting the desired oxygen diffusion. Goal of the present research is to reduce the electronic conductivity through incorporation of electron-trapping inclusions,[1–7] but without compromising the ionic conductivity. The present example uses gadolinium-doped ceria as the oxygen conductive phase and manganese/cobalt-doped alumina as the electron-trapping nano-inclusion. The Mn- and Co-oxide additions create the necessary electron-trapping sites at the interface. This novel solid-electrolyte concept should allow us to manufacture SOFC, which can be operated at significantly lower temperatures. Thus,

* Corresponding author.
E-mail address: giesche@alfred.edu (H. Giesche).

0955-2219/$ – see front matter © 2007 Elsevier Ltd. All rights reserved.
doi:10.1016/j.jeurceramsoc.2007.09.031

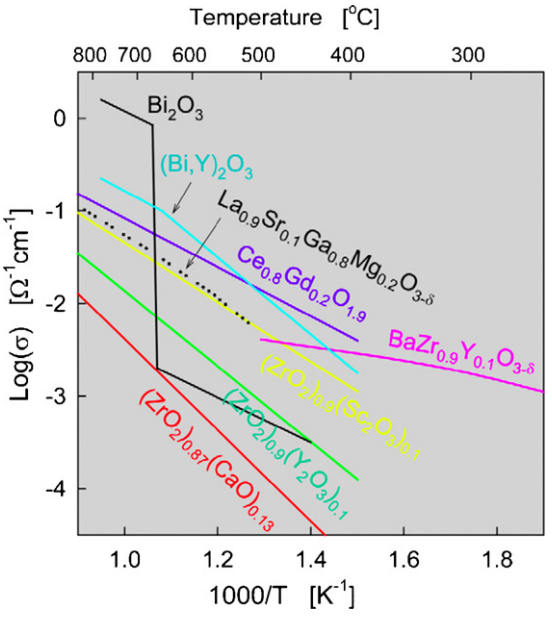

Fig. 1. Summary of conductivities of selected electrolyte materials.[10]

eliminating numerous other problems encountered in the present SOFC designs.

2. Experimental

2.1. Synthesis of coated nano-particulates and sintering

Reagent grade $Al(OC_4H_9)_3$, $Mn(NO_3)_2{\bullet}2H_2O$, $Co(NO_3)_2{\bullet}6H_2O$, $Ce(NO_3)_2{\bullet}6H_2O$, $Gd(NO_3)_2{\bullet}6H_2O$, and NH_4OH solution were obtained from Aldrich and used without further purification. All salts were pre-dissolved as 0.2 mol dm^{-3} stock-solutions.

Following the general procedure described by Yoldas,[8] alumina sols were prepared by adding 123 g aluminum alkoxide under vigorous stirring into 900 g water at 75 °C. After stirring for 30 min, 0.830 g conc. HNO_3 was added and the solution aged for an additional 5 days at 100 °C.

At that point 125 g of the alumina sol was used for the further coating process.

In about 100–200 ml of water 0.090 g of $Mn(NO_3)_2{\bullet}2H_2O$, 0.091 g of $Co(NO_3)_2{\bullet}6H_2O$, and approximately 1 g of a 28 wt.% ammonia solution were slowly added at 90 °C, stirred for 4 h and further aged for an additional 12 h.

Finally, in about 600–700 ml of water 20.74 g of $Ce(NO_3)_2{\bullet}6H_2O$, 5.388 g of $Gd(NO_3)_2{\bullet}6H_2O$, and approximately 4.5 g of a 28 wt.% ammonia solution were slowly added at 90 °C, stirred for 4 h and further aged for an additional 12 h.

Water was slowly evaporated at 100 °C and the powder pre-calcined at 900 °C for 4 h in air. The above described process yielded in an overall (theoretical) composition of 49.84 at.% Al, 0.68% Mn, 0.68% Co, 39.05% Ce, and 9.76% Gd (sample COAT-B).

Vice versa a composition with half the concentration for Mn and Co (sample COAT-C) was prepared as well as a 'simple' Gd-doped ceria with a 20/80 ratio (sample GdC).

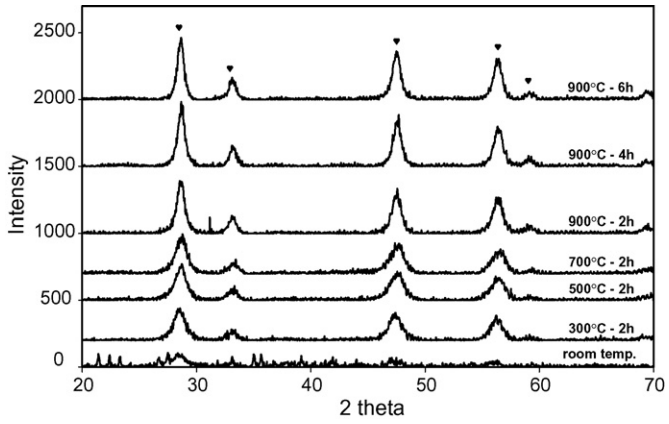

Fig. 2. XRD analysis of $Gd_{0.2}Ce_{0.8}O_{1.9}$–0.34Mn–0.34Co–Al_2O_3 (Coat-C) coated powder calcined at different temperatures starting from room temperature through 900 °C (♥represents $Gd_{0.2}Ce_{0.8}O_{1.9}$ matches with PDF card 01-075-0162).

After calcination, the powders were ground and sieved using a 75 μm mesh. Two to three grams of the powders were uniaxially die-pressed at 15 MPa pressure and then cold isostatically pressed at 200 MPa to form cylindrical green pellets of 3 mm height, 11 mm diameter.

The pellets were sintered (a) in a 'conventional' furnace at 2 °C/min heating rate to 1350 °C (5 h hold) followed by 2 °C/min cool-down, or (b) in a hybrid microwave furnace at 10 °C/min heating rate to 1350 °C (30 min hold) followed by 10 °C/min cool-down.

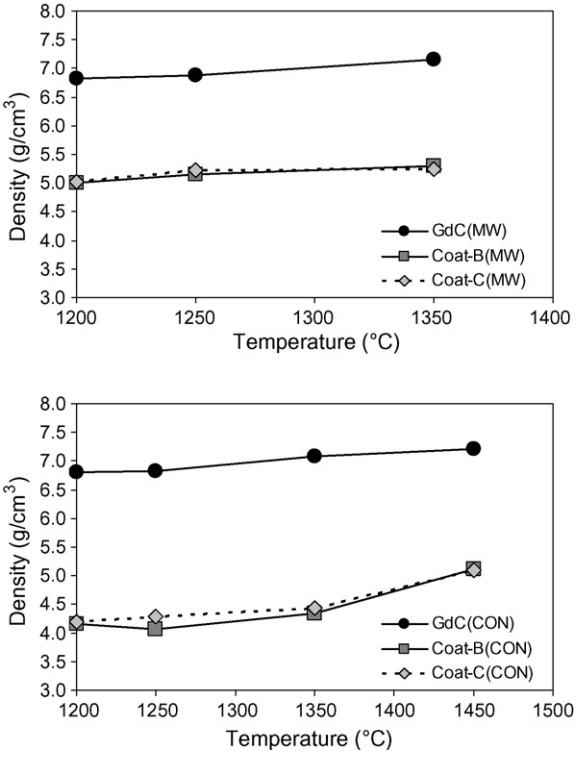

Fig. 3. Density of microwave (top) and conventionally (bottom) sintered samples.

2.2. Characterization

X-ray diffraction experiments were performed on a Philips, XRG 3100 X-ray generator. The X-ray generator was set to 40 kV and 20 mA current, utilizing Cu Kα radiation with a wavelength of 1.54 Å, from 20° to 70° (2θ), with a step size of 0.04° and count times of 4.0 s.

SEM analysis used an FEG 200 (FEI Company, Hillsboro, OR) environmental SEM (ESEM) with a field emission gun (FEG) operating at 10 kV. The energy-dispersive X-ray spectrometer (EDS) attached to the ESEM was used for chemical composition analysis. Powder samples were prepared by drying suspensions and in the case of sintered pellets, fracture surfaces were observed. Before analyzing all samples were coated with a 60:40 Au:Pd conductive layer in order to prevent charge build-up.

Table 1
Vickers hardness of samples

Sample ID	Vickers hardness (GPa), conventional sintered 1450 °C	Vickers hardness (GPa), microwave sintered 1350 °C
GdC	9.1	
Coat-C	7.2	9.8
Coat-B	9.2_5	10.1

Impedance spectroscopy was used in the frequency range between 1 Hz and 10 MHz using a Solartron 1260 impedance/gain analyzer along with a Centurion Qex furnace.

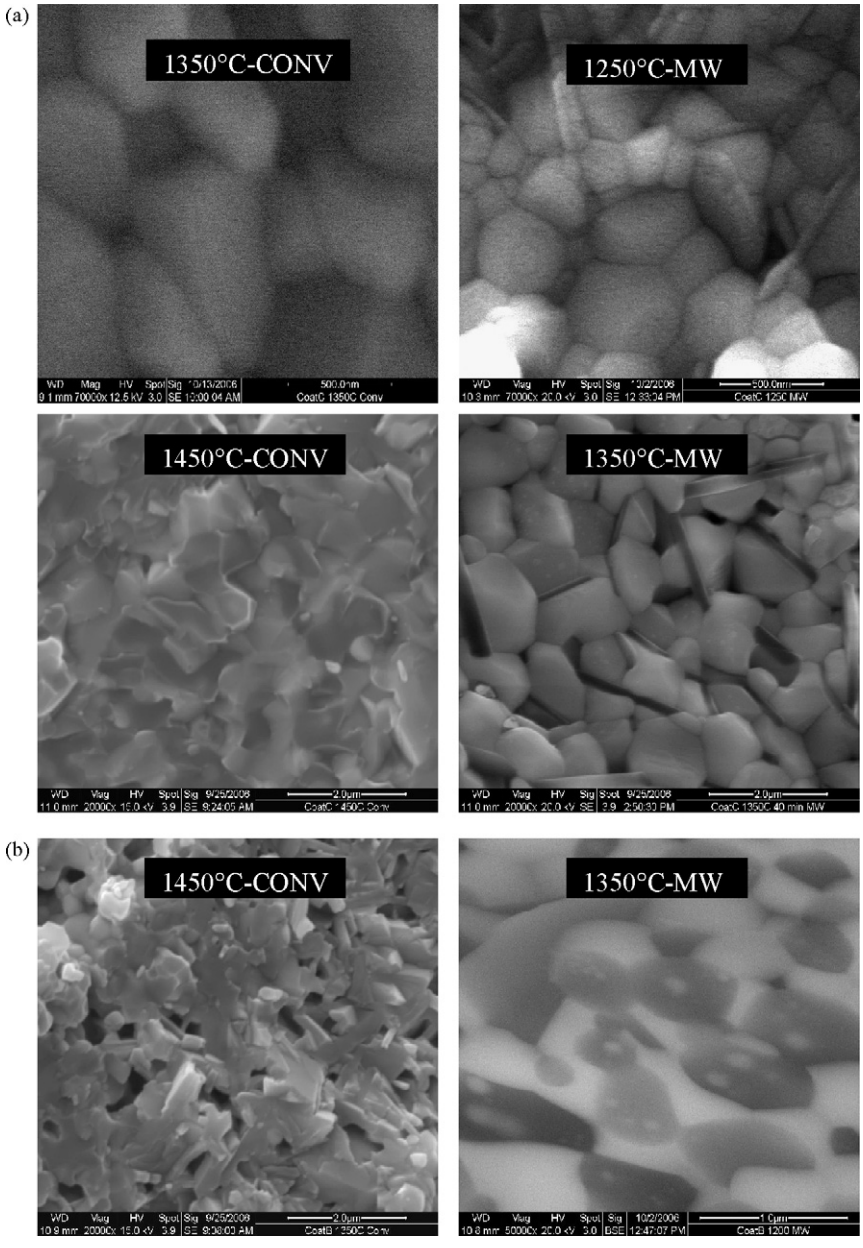

Fig. 4. (a) SEM micrograph of $Gd_{0.2}CeO_{0.8}$–0.34Mn–0.34Co–Al_2O_3 sintered sample. (b) SEM micrograph of $Gd_{0.2}CeO_{0.8}$–0.68Mn–0.68Co–Al_2O_3 sintered sample.

Sintered cylindrical specimens were coated on both faces with platinum ink A3788A (Engelhard, Lot #M34831) cured at 900 °C (30 min hold). Correction files were used to account for and eliminate any resistance due to the leads. All data were collected while sweeping from high to low frequency in order to avoid polarization in the sample. Nyquist plots were then generated at each temperature and analyzed in the Z-View software (Version 2.6 Scribner Associates Inc., Southern Pines, NC, 2002).

A Kepco power supply (55 V-2A max. set at 20 V) was used in combination with a Keithley Multimeter to measure 4-point dc conductivity. Sintered pellets were shaped into rectangular bars and electroded with platinum ink A3788A (Engelhard, Lot #M34831). Measurements were performed between 200 and 1000 °C (in air) and 500 and 1200 °C (controlled atmosphere). The oxygen pressure (10^{-30} to 10^{-2} atm) was controlled by using Ar–O_2 or CO–CO_2 mixtures. For each data point temperature, P_{O_2}-equilibrium was established before making the final measurement (indicated by a steady value of conductivity).

3. Results and discussion

3.1. Sintering

Effects of various synthesis parameters on the gadolinium-doped ceria particles and the coated alumina systems are described in more detail elsewhere.[9]

TGA/DTA experiments indicated an approximate weight-loss between 35 and 40 wt.% at a temperature of about 250 °C and some minor continued weight-loss until about 500 °C. The as-prepared powders were essentially amorphous. However, already at temperatures of 300 °C the $Gd_{0.2}Ce_{0.8}O_{1.9}$ phase was clearly noticed in XRD tests (see Fig. 2). The XRD peaks indicated only a minor increase in crystallite size as the calcination temperature was increased to 900 °C. No, alumina peaks were observed. Apparently the alumina core particle remains amorphous at calcination temperatures at or below 900 °C.

Density measurements, as shown in Fig. 3, demonstrated an advantage of microwave sintering, since the coated samples reached densities above 5.0 g/cm^3 at 1250 °C in the microwave sintering experiment, whereas 1450 °C was needed in the conventional sintering run. A precise value of the 'percent-theoretical density' is not possible due to the mixed composition of the material. However, judging from scanning electron micrographs, it appears that densities above 5.0 g/cm^3 would correspond to a theoretical density of at least 95%. The microwave temperature was measured with a thermocouple placed inside the insulation box about 2.5 cm from the actual sample. Nevertheless, one has to be very careful with any 'over-interpretation' of the temperature effects between the microwave and the conventional sintering due to the inherent difficulties in measuring the 'true' sample temperature.

In addition, microwave sintering leads to higher hardness values as demonstrated in Table 1. This effect can be explained by the smaller grain sizes, which are typically encountered in microwave sintering, due to the 'lower' sintering temperatures needed to reach a certain density, and the faster sintering cycle (30 min versus 5 h hold time at temperature). Fig. 4 shows micrographs of fracture surfaces for samples sintered at different temperatures. A submicron average grain size was observed for 1350 °C conventional and 1250 °C microwave sintered sample.

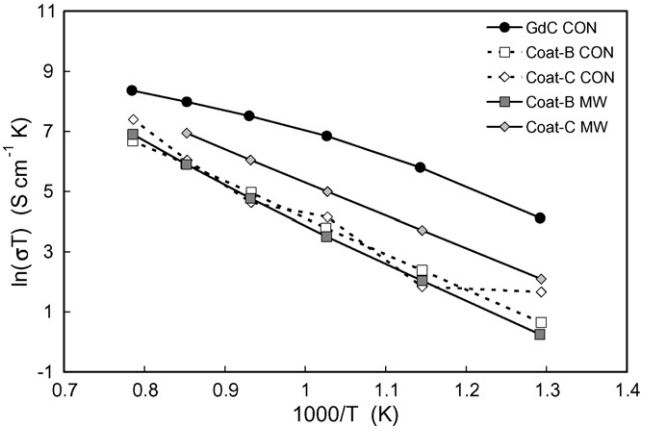

Fig. 5. Impedance spectroscopy in air ('ionic conductivity') between 400 and 1000 °C.

3.2. Conductivity

Adding gadolinium to ceria will create oxygen vacancies, which in effect will enhance the oxygen conductivity. How-

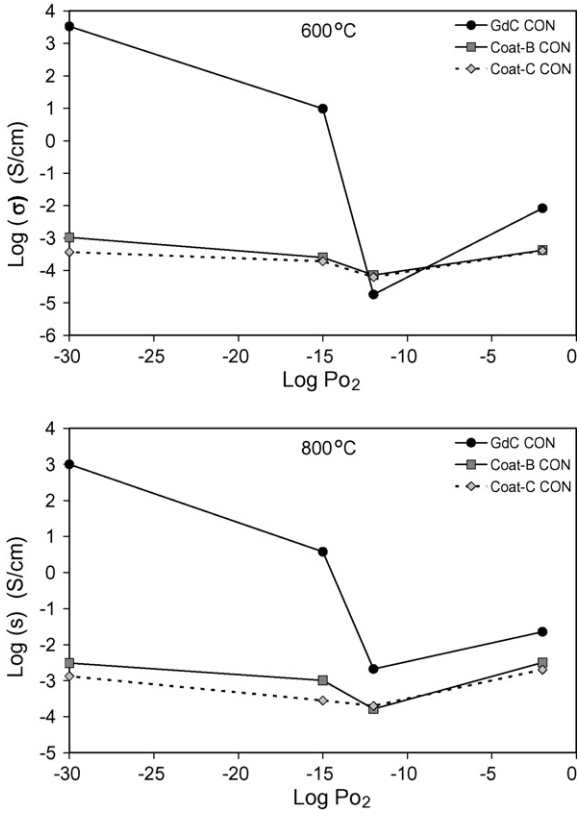

Fig. 6. Electrical conductivity as a function of oxygen partial pressure at 600 °C (top) and 800 °C (bottom).

ever, cerium ions can also under go a reduction from the +IV to +III oxidation state. The later process leads to electronic conductivity, which in effect will reduce the usefulness of the material as an oxygen ion conductor membrane, since it can lead to recombination effects in the SOFC. Measuring the conductivity in air (Fig. 5) is essentially due to ion conductivity only. It is not surprising that compared with the 'pure' gadolinium-doped ceria (GdC) the conductivity of the nano-composite samples are lower since 50 wt.% of the material is 'insulating' alumina. However, when the conductivity is measured at lower oxygen partial pressures (where electronic conductivity becomes more significant as seen by the increased conductivity below oxygen pressures of 10^{-15} for the pure GdC), it is obvious that the nano-composite suppresses the electronic conductivity as the conductivity remains low at around 10^{-3} to 10^{-4} S/cm and no electronic conductivity due to the Ce^{+IV} to Ce^{+III} conversion is detected (see Fig. 6).

On another note, it is interesting to notice that the conductivity of the pure gadolinium-doped ceria prepared in this study shows a higher ionic conductivity (by more than an order of magnitude) compared with data previously reported by Haile,[10] where a mixed oxide synthesis route was used.

4. Conclusions

The current examples show that electronic conductivity can be suppressed by the presence of electron-trapping inclusions/interfaces. In the current example, the manganese- or cobalt-doped alumina grains created those electron-trapping sites. The electron-trapping mechanism works only over a certain distance (depletion layer). Thus, it becomes obvious that a well-designed nano-composite is essential to optimize the effect. The present examples are a first step towards such a controlled microstructure. However, further improvements in the synthesis and sintering procedures are needed to utilize the effect to its fullest extent.

Acknowledgements

We would like to thank Prof. D. Edwards, G. del Regno and G. Wynik for their help with the conductivity measurements, the microwave sintering and the ESEM. This work was supported by the Center for Advanced Ceramic Technology (CACT) at Alfred University.

References

1. Dunn, D. G., The role of glass additives in zinc oxide varistors. M.S. Thesis. Alfred University, Alfred, NY, 1996.
2. Peterson, J. L., Effect of electron trapping on electronic and ionic conduction in cerium oxide/aluminum oxide composites. Ph.D. Thesis. Alfred University, Alfred, NY, 2003.
3. Morais, E. A. and Scalvi, L. V. A., Electron trapping of laser-induced carriers in Er-doped SnO_2 thin films. *J. Eur. Ceram. Soc.*, in press.
4. Fitting, H.-J., Cornet, N., Touzin, M., Goeuriot, D., Guerret-Piécourt, C. and Tréheux, D., Injection and self-consistent charge transport in bulk insulators. *J. Eur. Ceram. Soc.*, in press.
5. Touzin, M., Goeuriot, D., Fitting, H.-J., Guerret-Piécourt, C., Juvé, D. and Tréheux, D., Relationships between dielectric breakdown resistance and charge transport in alumina materials—effects of the microstructure. *J. Eur. Ceram. Soc.*, 2007, **27**(2/3), 1193–1197.
6. Seebauer, E. G. and Kratzer, M. C., Charged point defects in semiconductors. *Mater. Sci. Eng.: Rep.*, 2006, **55**(3–6), 57–149.
7. Kutty, T. R. N. and Ezhilvalavan, S., The influence of Bi_2O_3 non-stoichiometry on the non-linear property of ZnO varistors. *Mater. Chem. Phys.*, 1994, **38**(3), 267–276.
8. Yoldas, B. E., Alumina sol preparation from alkoxides. *Ceram. Bull.*, 1975, **54**(3), 289–290.
9. Chockalingam, R., Synthesis and characterization of Gd–CeO_2/Al_2O_3 nano-composite electrolyte for solid oxide fuel cells. M.S. Thesis. Alfred University, Alfred, NY, 2007.
10. Haile, S. M., Fuel cell materials and components. *Acta Mater.*, 2003, **51**, 5981–6000.